ELSEVIER

Polymer 43 (2002) 775–780

polymer

www.elsevier.com/locate/polymer

Generation of electrospun fibers of nylon 6 and nylon 6-montmorillonite nanocomposite

Hao Fong[a], Weidong Liu[b], Chyi-Shan Wang[c], Richard A. Vaia[d,*]

[a]*Universal Technology Corporation, Air Force Research Laboratory, Wright-Patterson Air Force Base, OH 45433, USA*
[b]*Systran Federal Corporation, Air Force Research Laboratory, Wright-Patterson Air Force Base, OH 45433, USA*
[c]*University of Dayton Research Institute, 300 College Park Avenue, Dayton, OH 45469, USA*
[d]*Air Force Research Laboratory (AFRL/MLBP), Material and Manufacturing Directorate, Wright-Patterson Air Force Base, OH 45433-7750, USA*

Received 30 July 2001; received in revised form 25 September 2001; accepted 27 September 2001

Abstract

Dissolution and reprocessing of exfoliated montmorillonite–nylon 6 (NLS) nanocomposite is demonstrated, illustrating the potential of using polymer nanocomposites as the foundation for fabricating nano- and mesoscopic structures, nanofibers in this case, and thus exerting hierarchical control of morphology and form through the combination of a nanostructured material and a nanoscale fabrication technique. Exfoliated morphology, present in the melt-fabricated NLS nanocomposite, was preserved in cast films and electrospun fibers from hexafluoroisopropanol solution. However, addition of a few percent *N*,*N*-dimethyl formamide resulted in agglomeration of the dispersed montmorillonite layers and an overall mixed morphology, demonstrating solvent partitioning and the delicate enthalpic balance necessary to maintain layer dispersion. Fibers and nanofibers of NLS nanocomposite (diameters between 100 and 500 nm) were electrospun from solution, and collected as non-woven fabrics, or as aligned yarns. Together with these cylindrical shaped fibers and nanofibers, ribbon shaped fibers (width ~ 10 μm, thickness ~ 100–200 nm) were also found in the products. The electrospinning process resulted in highly aligned montmorillonite layers (layer normal perpendicular to the fiber axis) and nylon 6 crystallites (layer normal parallel to fiber axis). © 2001 Published by Elsevier Science Ltd.

Keywords: Electrospinning; Nanocomposite; Nanofiber

1. Introduction

The utility of polymer nanocomposites (PNCs) is widely acknowledged [1]; however many times, traditional large-scale processing approaches are not capable of achieving or maintaining optimal nanoscopic dispersion of the fillers, and thus delivering the potential suite of property enhancements espoused by many PNC reports. Beyond the challenges of traditional processing, the potential to fabricate and process micro- and nanoscale structures from PNCs and the determination of analogous property enhancements is relatively unexplored. In these regards, the reformulation of previously fabricated PNCs such that the desired morphological characteristics are maintained would be of substantial interest. For example, dissolution of melt-compounded pellets of PNC would enable alternative approaches to coating, film and fiber fabrication.

Electrospinning is a straightforward way to produce polymer nanofibers from solution [2–4]. In electrospinning, a polymer solution is suspended and stabilized by its surface tension. Charges are induced on the liquid droplet by an electric field. As the intensity of the electric field increases, the droplet elongates until a critical value at which the electrostatic force overcomes surface tension and a charged jet of the solution is ejected. As the jet travels, the solvent evaporates, leaving behind a charged polymer fiber. Continuous fibers can be collected either in the form of non-woven fabric, or as aligned yarns [2–4]. Electrospun fibers have unusually small diameters, ranging downward from typical textile fibers by as much as three orders of magnitude. The subsequent ultra-large surface–volume ratio of these fiber mats is of great interest for reinforced composites, filtration, protective clothing, biomedical applications including wound dressing, and as supports for enzymes or catalysts [5].

In the process of electrospinning, the phenomenon of bending instability results in the electrospinning jet being elongated up to 100,000 times in a short distance and in less than one second [6]. This extremely large effective draw ratio will likely align anisotropic nanofillers, such as

* Corresponding author. Tel.: +1-937-255-9184; fax: +1-937-255-9157.
E-mail address: richard.vaia@afrl.af.mil (R.A. Vaia).

0032-3861/02/$ - see front matter © 2001 Published by Elsevier Science Ltd.
PII: S0032-3861(01)00665-6

dispersed layered silicates or carbon nanotubes, as well as extend polymer chain conformations and influence the formation and structure of polymer crystallites.

Many reports have examined the morphology development of polyamides during spinning, motivated by its importance as a synthetic fiber [7–12]. For example, previous work by Murase and coworkers [7] showed the crystal structures of nylon 6 (α- and γ-form) depends on the fiber formation process (take-up speed). Overall, the structure of the as-spun nylon 6 fibers depends markedly on process conditions such as temperature, take-up speed, humidity and molecular weight.

Literature discussion of melt or solution spinning of polyamide nanocomposites though is sparse. Similarly, only a few direct morphological investigations (microscopy and scattering) of the development of the morphology of the nanofillers in shear or elongation flow are available. Previous work by Kojima et al. [13,14] examining the morphology of 60 μm films and 5 mm injection molded bars indicated that preferential orientation of the silicate layers result from shear flow and the presence of hard boundaries (mold wall). Additionally, coupling between the layered silicate and polymer lead to preferential orientation of the polymer crystallites. Recent work by Medellin-Rodriguez et al. [15] imply that the mechanism for layer alignment in a shear flow is more complex than initially assumed, resulting in a fraction of the layers aligned normal to the shear direction. Finally, Giza and coworkers [16], examining the high-speed, melt-spinning of nylon 6 nanocomposites with birefringence, found that at lower take-up speeds (1–3 km/h), orientation (birefringence) of the nanocomposite fibers were greater than the orientation of neat nylon, however at higher take-up speeds (>4 km/h) it was less. Overall, differences in crystallization, crystal form, density, and fiber properties (modulus and tenacity) were partially attributed to the influence of the silicate layers on the nucleation of oriented inter-crystalline regions of polymer.

Herein, the ability to dissolve nylon 6–montmorillonite nanocomposites (NLS), initially fabricated by melt processing, and to reformulate into electrospun nanofibers, which maintains the nanoscale dispersion of the montmorillonite, is demonstrated. This illustrates the potential of using PNCs as the foundation for fabricating nano- and mesoscopic structures, nanofibers in this case, and thus exerting hierarchical control of morphology and form through the combination of a nanostructured material and a nanoscale fabrication technique. Furthermore, electrospinning of PNCs provides additional insight into the coupling between processing and silicate layer alignment, polymer chain orientation and polymer crystal phase development.

2. Experimental

Neat nylon 6 and nylon 6 with 7.5 wt% Closite 30B (bis(2-hydroxy-ethyl) ammonium montmorillonite) (NLS) were received from Southern Clay Products, Inc., in the form of extruded films and pellets. Fabrication details can be found in Refs. [17,18]. The initial, unintercalated layer repeat distance (*d*001) for the as received, dried (vacuum, 70°C for 12 h) and solvent suspended and dried (3% solution in 1,1,1,3,3,3-hexa-fluoro-2-propanol (HFIP), cast at room temperature for 48 h and vacuum 70°C for 12 h) 30B was 1.8 nm. HFIP and *N*,*N*-dimethyl formamide (DMF) were used as received from Aldrich.

Ten percent by weight solutions of nylon or NLS were prepared using pure HFIP or a mixture of 95% HFIP and 5% DMF by adding extruded films to the solvent and stirring for 12 h before use. HFIP is an excellent solvent for nylon and much easier to evaporate than other nylon solvents, such as formic acid/*meta*-cresol. Although DMF is a non-solvent for nylon, empirically it has been found to be helpful during the electrospinning and the formation of electrospun fibers. Solvent blending of nylon 6 and Closite 30B were conducted via combining nylon 6/HFIP and Closite 30B/HFIP solutions. Closite 30B did not disperse well in HFIP and solutions were sonicated with a horn sonicator before mixing with the polymer solution to facilitate particle dispersion. Cast films were formed at room temperature under vacuum for 12 h.

The electrospinning apparatus used a high voltage power supply (ES30P, 200 μA at 30 kV, from Gamma High Voltage Research, Ormond Beach, Florida). A positive high voltage was applied, through a copper wire, to the solution inside a glass pipette. A grounded metal sheet was placed 25 cm below the tip of the glass pipette. Several glass microscope slides covered by films of evaporated graphite were placed on the metal sheet. The pipette was tilted a few degrees from the horizontal so that surface tension maintained a small droplet of the solution at the tip. As the electrical potential was gradually increased to 20 kV, a jet was created. The jet, formed by electrical forces, followed a complicated stretching and looping path as it dried and solidified. Non-woven fabrics were formed on the surface of aluminum foil that was covered on the grounded metal sheet. Aligned yarns can be collected by rapidly oscillating a grounded frame within the jet.

A Philips CM-200 TEM with a LaB_6 filament operating at 200 kV and a XL30 SEM (Philips Electron Optics, Inc., Hillsboro, OR) was employed for microscopy. The X-ray diffraction measurements were carried out with a rotating anode X-ray generator (50 kV and 250 mA; pin hole collimator 0.0508 mm) with Cu Kα radiation ($\lambda = 1.54$ Å) using an image plate (8×10.5 mm^2) at 72 mm from the sample. WAXD images were obtained using Storm 820 Scanner (Molecular Dynamics Inc.). The curves of integrated intensity vs 2θ for the deconvolution of the superposition of crystalline peaks and broad amorphous halo were obtained using Image Tool (The University of Texas Health Science Center in San Antonio). Deconvolution was carried out using GRAMS/32 Spectral Notebase (Galactic Industries Corporation) with Gaussian peak shape. The degree of crystallinity is the ratio of the total

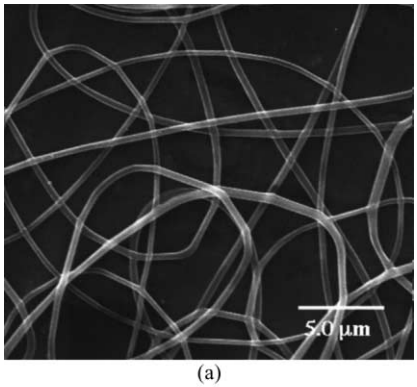

(a)

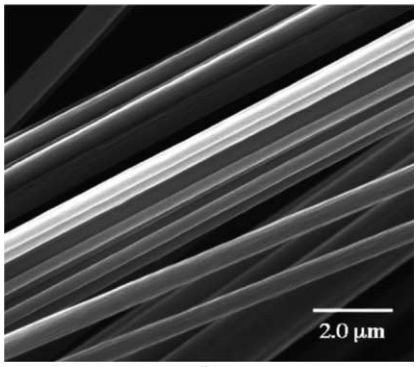

(b)

Fig. 1. SEM images of the electrospun fibers from nylon 6 and NLS, in the form of (a) non-woven fabric and (b) aligned yarn.

intensity of nylon crystalline reflections to the total observed crystalline and amorphous intensities.

Thermal analysis was conducted by a DSC 2910 (TA Instruments). About 8 (±0.5) mg sample was crimped in an aluminum pan and heated at a rate of 10°C/min from room temperature to 280°C in a nitrogen atmosphere. The samples were dried at room temperature under high vacuum before DSC experiment. The degree of crystallinity was calculated by subtracting the non-reversible heat flow from the reversible heat flow and divided by the heat of crystallization of nylon 6 (190 J/g) [19].

3. Results and discussion

The electrospun nylon 6 and NLS fibers and nanofibers had diameters between 100 and 500 nm. Fig. 1 shows the appearance of the fibers either in the form of non-woven fabric (a) or as an aligned yarn (b). Morphologically (via SEM), the electrospun fibers of nylon 6 and NLS were nearly indistinguishable. Also, the solvents (HFIP or HFIP/DMF blend) had little effect on fiber size.

Among the electrospun products, some ribbon shaped fibers were also observed, from both the HFIP and the HFIP/DMF solutions. As shown in Fig. 2, the ribbon shaped fibers had a thickness of 100–200 nm and a width of ~10 μm. Both neat nylon 6 and the nanocomposite could form such ribbons. Ribbons have also been reported for

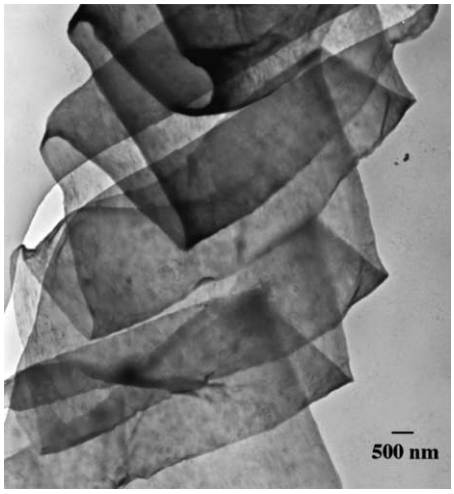

Fig. 2. Bright field TEM image of a ribbon shaped nanofiber.

electrospinning of elastin [20]. Rapid solvent removal from the surface of the jet presumably forms a skin, reducing subsequent solvent evaporation. This skin may cause the formation of hollow tubes, which subsequently collapse to form ribbons. Details of the mechanism of formation of ribbons require further investigation.

X-ray diffraction patterns of a solution cast film of nylon 6 (left) and an electrospun aligned yarn of nylon 6 (right) are shown in Fig. 3. The two diffraction rings in the solution cast film arise from the (200) and (002), (202) planes of the α-crystalline form of nylon 6. Crystallization in the solution cast sample does not exhibit any preferential orientation (uniform diffraction rings). In contrast, for the aligned electrospun yarn, the crystal structure of nylon 6 adopts the metastable γ-form (equatorial reflection: (001), (200); meridian reflection: (020)), with the layer normal of the crystallites was parallel to the fiber axis. These results are consistent with previous results that the γ-form is preferred in both as spun and spun drawn fibers of neat nylon 6 [12].

The X-ray diffraction patterns for films and fibers of NLS are summarized in Fig. 4. Film casting of solution-blended nylon 6 and Closite 30B yield an unintercalated nanocomposite (Fig. 4(a)). Nylon 6 chains are not incorporated within the montmorillonite tactoids, which remain aggregated (central ring, (001) of 30B, 1.7 nm). The small decrease in gallery height may be due to the de-intercalation of excess ammonium modifier (cation exchange capacity of 30B ~92 mequiv.; milli-equivalent exchange ratio of 30B ~95 mequiv.) and dissolution with in the polymer matrix. The α-crystal structure of nylon 6 dominates. In contrast, film casting of reconstituted, melt-processed NLS in HFIP results in an exfoliated nanocomposite (Fig. 4(b), absence of basal reflection of 30B). Consistent with previous reports on the melt-development of crystalline regions of nylon 6 in the presence of dispersed montmorillonite [13,14,17,21], the presence of dispersed 30B favors the formation of unoriented, metastable γ-phase during nylon 6 crystallization from solution. When DMF is added to HFIP, the

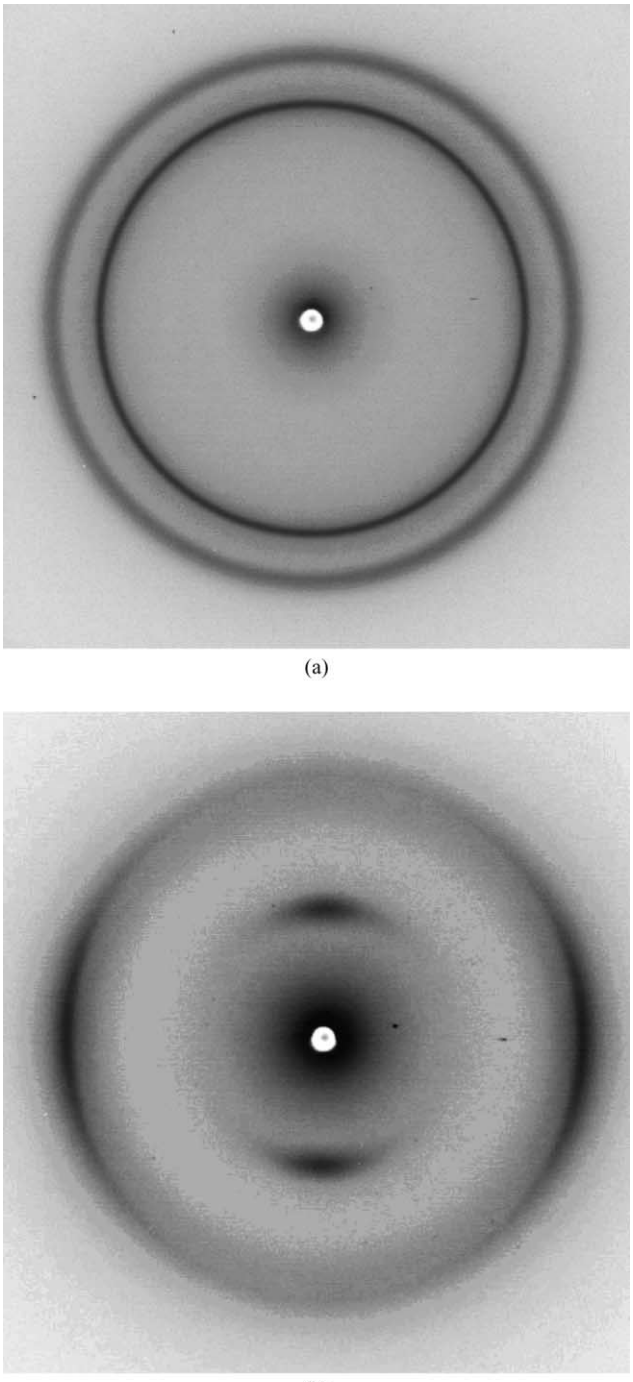

(a)

(b)

Fig. 3. X-ray diffraction patterns of neat nylon 6: (a) solution cast film, (b) electrospun aligned yarn (fiber axes verticle).

dispersion of the layered silicates collapses (central ring, Fig. 4(c), $d001 \sim 3.46$ nm), yielding intercalated montmorillonite aggregates.[1] As with the solution blended film, α-phase polymer crystallites dominate. This series of solution prepared films indicates that increased layer dispersion and associated interfacial area favors formation of γ-phase crystalline polymer whereas layer aggregation favors α-phase formation.

The stark difference in the layered silicate morphology between reconstituted melt-processed NLS and solution blended underscore the importance of process history and the crucial balance of interfacial interactions between the layered silicate and the surrounding medium. With regard to the reconstituted melt-processed NLS, initial exfoliation of 30B in the nylon 6 melt presumably results in strongly physi-absorbed or hydrogen-bonded nylon 6 chains at the montmorillonite surface and layer edge. Specifically, amide and carbonyl groups on the polymer probably associate with the oxygen plane of the layer surface and the weakly acidic SiOH and strongly acidic bridging hydroxyl groups present at the layer edge. Upon addition of HFIP, the physi-absorbed nylon chains are not displaced, and thus HFIP effectively disperses the individual montmorillonite layers by dissolution of the surface-absorbed nylon chains. However, the addition of DMF provides a competitive hydrogen-bond acceptor (aldehdye) for the amide linkage of the polymer to those sites available on the aluminosilicate layer, as well as a polarizable molecule with a high dielectric constant that would favor the charged silicate surface. Thus relatively small additions of DMF will preferentially partition within the system and lead to desorption of the nylon 6 chains from the aluminosilicate surface and subsequent layer aggregation (phase separation). In the contrasting case of solvent blending, the unfavorable interaction between HFIP and 30B does not initially provide substantial surface area for nylon 6 physi-absorption and thus layer dispersion does not occur. Also note that the interfacial interactions (30B–polymer) for the room temperature processed (solvent-blending) systems differ in an unknown manner from that of systems experiencing elevated temperature (>170°C) processing steps (melt processed), since the organic surface modifiers have a finite thermal stability at the montmorillonite surface [22,23].

Electrospinning of NLS from HFIP solution (Fig. 4(e)) yields fibers and nanofibers, which maintain the montmorillonite dispersion and contain highly oriented γ-phase crystalline polymer, similar to that observed for the electrospun nylon 6. The presence of the equatorial streak near the beam stop implies that the dispersed layered silicate is oriented with the layer normal perpendicular to the fiber axis. Note that the presence of the dispersed layers yield strong small angle scattering that masks small angle features that arise from the polymer crystallites [17,24]. The nonwoven fabric shows features comparable to the aligned yarn, albeit unoriented (Fig. 4(d)). As with the cast films, addition of DMF also collapses layer dispersion in the electrospun NLS fibers (Fig. 4(e)). The layer spacing within the aggregate though is smaller than observed in the solution cast films. The reason for this is not understood.

[1] Direct determination of the interlayer composition of the intercalated system via comparison of the layer repeat distance of the original unintercalated 30B (1.8 nm) is difficult because of unknown thermal history of the NLS and associated thermal degradation of the organic modifiers [22,23].

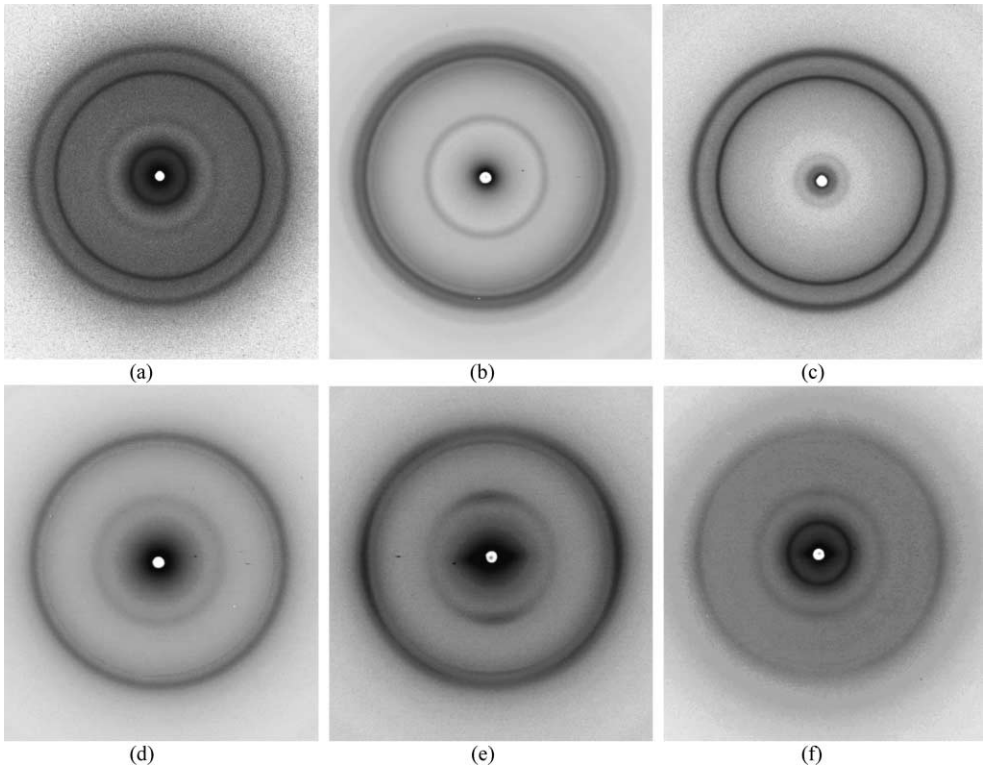

Fig. 4. X-ray diffraction patterns of NLS with different processing histories. Solution cast films of: (a) solution blended nylon 6 and closite 30B, (b) melt-processed NLS dissolved in HFIP, and (c) melt-processed NLS dissovled in HFIP/DMF mixture. Electrospun products of: (d) NLS from HFIP (non-woven fabric), (e) NLS from HFIP (aligned yarn), and (f) NLS from HFIP/DMF mixture (non-woven fabric).

γ-Phase nylon crystallites with the layer normal parallel to the fiber axis are prominent in all the electrospun products. This contrasts the solution prepared films, implying shear history as well as polymer–silicate interfacial area must be considered when discussing the origin of γ-phase crystallites. Note that the orientation of the polymer crystallites and montmorillonite layers are mutually orthogonal and thus indicate that a fraction of the nylon 6 chains are parallel to the montmorillonite surface.

Among the electrospun products, fibers with diameters less than 100 nm enabled direct imaging with TEM of the interior morphology of the fibers. Since the bending instability happens during the electrospinning, the non-woven fabric is a very uniform representation of fiber morphology. The TEM images in Fig. 5 were obtained by electrospinning non-woven fabric onto a Cu sample grid. Overall, the microscopy is consistent with the XRD observations. The montmorillonite layers are aligned along the fiber axis (dark lines: ~1 nm thick, montmorillonite layers viewed parallel to the layer edge). For HFIP solutions, individual, exfoliated montmorillonite layers dominate the morphology. In contrast, for the HFIP/DMF solution, a large percentage of stacks of montmorillonite layers are observed along with individual layers. This mixed morphology has been observed in various other PNC systems [24].

Table 1 summarizes the degree of polymer crystallinity determined by XRD and DSC for various films and electrospun fibers. Similar trends in crystallinity are observed for both techniques. The addition of layered silicate substantially decreases the fractional crystallinity developed during solvent removal for the cast films. Overall electrospinning, whether neat nylon or NLS, results in reduced crystallinity relative to the solution cast film of neat nylon 6. This contrasts the increased crystallinity observed by Giza and coworkers for high-speed, melt-spinning of nylon 6 nanocomposite fibers [16]. Although the ultra-large draw ratio in electrospinning should produce greater chain alignment,

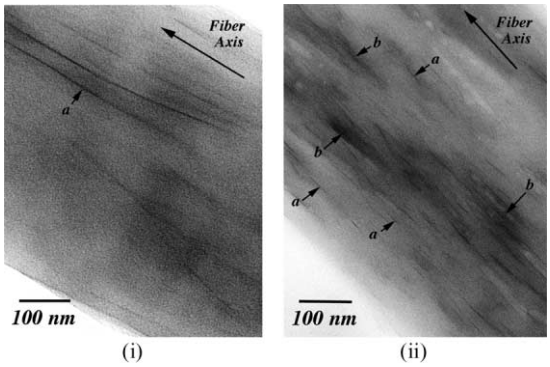

Fig. 5. Bright field TEM images of the electrospun nanocomposite nanofibers from (i) pure HFIP solution, (ii) HFIP 95%/DMF 5% solution (a: single sheet, b: stacked sheets/tactoids).

Table 1
Comparison of measured crystallinity from WAXD and DSC

	Fractional crystallinity				
	Films		Electrospun nanofibers		
	Nylon 6 (HFIP)	NLS (HFIP)	Nylon 6 (HFIP)	NLS (HFIP)	NLS (HFIP/DMF)
WAXD	0.362	0.2312	0.2361	0.2316	0.2316
DSC	0.3578	0.2346	0.2817	0.2772	0.2472

concomitant rapid solvent removal inhibits formation of perfect crystallites in the as-spun nanofibers.

4. Conclusions

Reformulation of exfoliated NLS nanocomposite is demonstrated and fibers, ribbons and nanofibers were electrospun from solution into non-woven fabrics or aligned yarns. The electrospinning process resulted in highly aligned montmorillonite layers (layer normal perpendicular to the fiber axis) and nylon 6 crystallites (layer normal parallel to fiber axis). The ultra-large draw ratio and rapid solvent removal of electrospinning (as well as the addition of the montmorillonite layers) favors the formation of γ-phase nylon crystallites in pure nylon 6 and NLS fibers. The addition of a few percent DMF to the solutions resulted in agglomeration of the dispersed montmorillonite layers and an overall mixed morphology, demonstrating solvent partitioning and the delicate enthalpic balance necessary to maintain layer dispersion. Future efforts will examine the utility of electrospinning to align other nanofillers such as carbon nanotubes.

Acknowledgements

The US Air Force Office of Scientific Research and Materials and Manufacturing Directorate supported this work. The authors are grateful to Southern Clay Products for supplying the neat Nylon 6 and nylon 6/montmorillonite nanocomposite.

References

[1] Pinniavaia TJ, Beall G, editors. Polymer clay nanocomposites. New York: Wiley, 2001.
[2] Reneker DH, Chun I. Nanotechnology 1996;7:215.
[3] Fong H, Chun I, Reneker DH. Polymer 1999;40:4585.
[4] Fong H, Reneker DH. J Polym Sci B 1999;37:3488.
[5] Fong H, Reneker DH. Structure formation in polymeric fibers. In: Salem DR, Sussman MV, editors. Electrospinning and formation of nanofibers. Munich: Hanser, 2001. Chapter 6.
[6] Reneker DH, Yarin AL, Fong H, Koombhongse S. J Appl Phys 2000;87:4531.
[7] Murase S, Kashima M, Kudo K, Hirami M. Macromol Chem Phys 1997;198:561.
[8] Ziabicki A, Kedzierska K. J Appl Polym Sci 1959;2:14.
[9] Ziabicki A, Kedzierska K. J Appl Polym Sci 1962;6:111.
[10] Ishibashi T, Aoki K, Ishii T. J Appl Polym Sci 1970;14:1597.
[11] Bankar VG, Spruiell JE, White JL. J Appl Polym Sci 1977;21:2341.
[12] Murthy NS, Aharoni SM, Szollosi AB. J Polym Sci B 1985;23:2549.
[13] Kojima Y, Usuki A, Kawasumi M, Okada A, Kurachi T, Kamigaito O, Kaji K. J Polym Sci: Polym Phys 1995;33:1039.
[14] Kojima Y, Matsuoka T, Takahasi H, Kurachi T. J Appl Polym Sci 1994;51:683.
[15] Medellin-Rodriguez FJ, Burger C, Hsiao BS, Chu B, Vaia R, Phillips S. Polymer 2001;42:9015.
[16] Giza E, Ito H, Kikutani T, Okui N. J Macromol Sci Phys B 2000;39:545.
[17] Lincoln DM, Vaia RA, Wang Z-G, Hsiao BS. Polymer 2001;42:1621.
[18] Cho JW, Paul DR. Polymer 2001;42:1083.
[19] Inoune M. J Polym Sci A 1963;1:2697.
[20] Huang L, McMillan RA, Apkarian RP, Pourdeyhimi B, Conticello VP, Chaikof EL. Macromolecules 2000;33:2989.
[21] Lincoln D, Vaia RA, Wang Z-G, Hsiao BS, Krishnamoorti R. Polymer 2001;42:9975.
[22] Xie W, Gao Z, Pan WP, Singh A, Vaia RA. Chem Mater 2001;13:2979.
[23] Van DerHart V, Gilman J. Submitted for publication.
[24] Vaia RA. In: Pinniavaia TJ, Beall GW, editors. Polymer clay nanocomposite. New York: Wiley, 2000.